Silicon (2023) 15:7685–7703
https://doi.org/10.1007/s12633-023-02629-7

REVIEW

A Review on Waste Glass-based Geopolymer Composites as a Sustainable Binder

Datla Neeraj Varma[1] · Suresh Prasad Singh[1]

Received: 20 June 2023 / Accepted: 11 August 2023 / Published online: 21 August 2023

Abstract
Waste glass (WG) is one of the major constituents of municipal solid waste, rich in amorphous silica.. The present article comprehensively reviews the geopolymer materials synthesized with waste glass powder (WGP) as one of the precursors. The fresh, hardened and durability properties of the material are appraised, emphasizing the effect of synthesis parameters. The embodied energy and the embodied CO_2 in WGP-based geopolymer are presented to highlight its sustainability. The workability and setting times of the geopolymer are highly influenced by the surface properties of the glass particle. A certain dosage of WGP significantly improves the mechanical and durability properties of the geopolymer. Further, other synthesis parameters such as the type of co-precursor, the particle size of WGP, the type of alkali activator and its concentration, and the liquid activator to solid binder ratio also cause predominant changes in the material properties. Durability studies on WGP-based geopolymers are limited, particularly the quantification of alkali-silica reactions and resistance towards chemical attacks. In addition, advanced sustainable studies are essential for promoting WGP-based geopolymer as a sustainable material. Overall, previous studies indicate the effective incorporation of WGP as a precursor material because of its relatively better performance than other cementitious materials. This review gives the researchers and field engineers a better understanding of utilizing WGP as a precursor in the synthesis of geopolymer.

Keywords Waste glass recycling · Geopolymerization · Fresh and hardened properties · Durability and sustainability

1 Introduction

Glass is an ever-present material in the current society. Since its inception in the nineteenth century, glass production has increased drastically. In 2007, glass production was about 89.4 million tons around the world [1]. It is available in the form of panels, bottles, glasses, containers etc. The universal production of glass materials (containers and bottles) was raised to about 689.94 billion units in 2020. It is forecasted to be 922.43 billion units by 2026 [2]. Despite wide applications, after its usage or service life, a huge quantity of glass is being treated as waste material and disposed-off along with other municipal solid wastes in landfills without re-use [3]. It is due to the inert, non-combustible and non-biodegradable nature of the glass [4]. Globally, 200 Mt of WG is generated every year, which accounts for 5% of total solid waste [5]. However, the average recovery rate is limited to 31.3% [6]. The statistical data on WG generation and recovery rate for various countries are listed in Table 1. Although few countries have a better recovery rate of WG, its usage for glass production is limited due to the challenges in the segregation and decoloring process of colored WG [13]. In this scenario, it is essential to explore new paths for re-use of WG.

In the construction industry, alkali activation of aluminosilicate-rich materials is a novel technique to produce a sustainable green binding material termed as geopolymer [14]. It is synthesized from industrial waste products containing amorphous silica and alumina in the presence of an alkali medium at low temperatures, i.e. less than 100 °C [15, 16]. At present, significant literature is available on geopolymer synthesized from slag, fly ash (FA), rice husk ash (RHA), metakaolin (MK), silica fume, bottom ash, waste cement concrete (WCC), etc. and their blends [17–26]. These geopolymer materials possess high-strength properties with

✉ Suresh Prasad Singh
spsingh@nitrkl.ac.in

Datla Neeraj Varma
519ce1015@nitrkl.ac.in

[1] Department of Civil Engineering, National Institute of Technology Rourkela, Rourkela, India

Table 1 WG generation and recovery rate for various countries

Country	WG generation (Mt/year)	Recycling rate (%)	Year	Reference
European Union	18.5	79%	2014	[4]
USA	12.25	25%	2012	[3]
China	40.0	13%	2010	[7]
Egypt	3.45	16%	2011	[8]
Australia	1.16	59%	2018	[9]
India	0.85	47%	2015	[10, 11]
Canada	0.39	68%	2018	[8, 12]

low creep and shrinkage; high resistance to acidic and fire attacks [27–36]. Further, geopolymer concrete reduces carbon dioxide (CO_2) emissions by up to 75% compared to ordinary Portland cement (OPC) concrete [27, 37]. Hence, geopolymer is considered as an alternative to conventional OPC.

In recent times, waste glass powder (WGP) has been used as a raw material in the manufacturing process of geopolymer. Few studies synthesized geopolymers with pure WGP alone and reported the formation of aluminosilicate hydrates [38, 39]. However, waste glass powder-based geopolymer (WGPG) attains low performance compared to slag/FA/MK geopolymer [4, 40]. Hence, the presence of other aluminosilicate precursors with WGP is essential. In this context, several laboratory studies confirmed the replacement of conventional precursors with WGP up to a certain extent [13, 38, 41–45]. It also eliminates the usage of silicate-base alkalis, which consume high energy during the production stage in geopolymer synthesis [46–48]. Thus, the geopolymer technique can be effectively used to recycle WG with high economic benefits.

This review paper presents the evolution of WGP as a precursor in geopolymer synthesis over time (Fig. 1). The improvements and limitations in the usage of WGP in geopolymer production are overviewed. The variations in fresh, hardened and durable properties of WGP-based geopolymer (WGPG) with varying synthesis parameters are discussed. The leaching of heavy metal ions from the WGPG and its sustainability are also highlighted.

2 Characteristics of WGP

2.1 Chemical Composition

At present, various glass materials such as soda-lime, borosilicate, alumina-silicate, lead, liquid crystal display (LCD) and barium glasses are available with varying chemical compositions pertinent to various applications [49, 50]. Table 2 summarizes the chemical composition of various WGP used in cementitious materials based on the type of the material and its color. The majority of the glass materials contain silica (55% to 72%), sodium (12–16%) and calcium oxides (5–12%) as major components, with minor alumina oxides (1% to 3%) [57]. However, alumina oxide (16.7%) appears as one of the major components in LCD glass. Meanwhile, no significant variation in the chemical composition is observed with color change. In addition, Fig. 2 presents the chemical compositions of soda lime WGP and other commonly used cementitious materials. It can be observed that the WGP has superior silica components with low alumina and calcium components compared to other aluminosilicate materials. Hence, WGP can be considered as a silica source for geopolymer materials.

2.2 Basic Structure

The schematic representation of the glass structure is portrayed in Fig. 3. It shows that the glass structure is mainly composed of silica ions, hence, treated as network formers. The alkali ions, such as sodium and calcium, modify the structure of the glass by compensating the negative charge with a positive charge around them, thus, being treated as

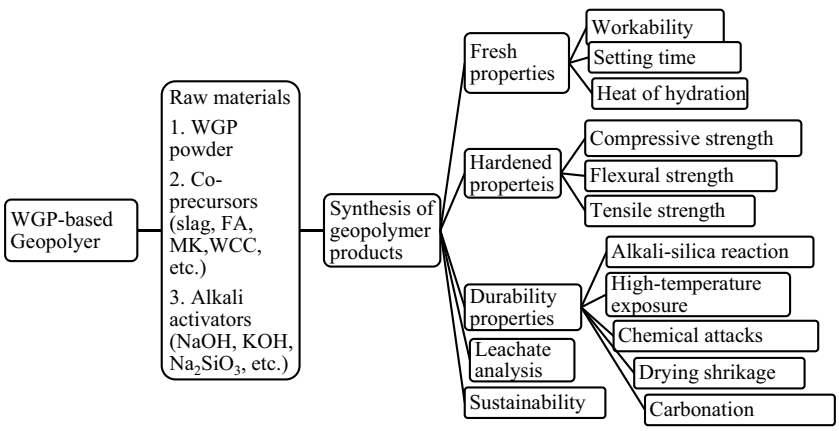

Fig. 1 Schematic diagram of different properties of WGP-based geopolymer (WGPG) discussed in this review

Table 2 Chemical composition of a variety of WGP

Type of WGP	Chemical composition												Reference
	SiO_2	Al_2O_3	Na_2O	MgO	Fe_2O_3	CaO	K_2O	TiO_2	PbO	SO_3	P_2O_5	BaO	
Soda-lime	72.43	1.24	10.81	0.69	0.43	13.43	0.45	-	-	0.11	-	-	[42]
LCD	62.48	16.67	0.64	-	9.41	2.70	0.20	0.01	-	-	0.01	-	[51]
Flurosent	58.39	1.92	15.30	2.60	0.16	11.69	1.04	-	-	0.13	7.85	-	[52]
Borosilicate	81.00	2.00	13.19	1.65	0.50	10.10	0.61	-	-	0.40	-	-	[53]
Lead	55.05	3.67	6.65	1.74	0.37	3.64	6.87	-	16.42	-	-	3.48	[54]
Color													
Colorless	72.68	1.57	10.60	1.69	0.78	11.84	0.50	-	-	0.27	-	-	[1]
Brown	71.19	2.38	13.16	1.70	0.29	10.38	0.70	-	0.15	0.04	-	-	[55]
Green	71.12	1.17	13.17	3.01	0.24	10.02	0.19		0.07	0.25	-	-	[55]
Mixed	68.33	1.93	14.65	1.30	0.36	11.90	0.70	0.06	0.05	0.09	-	0.06	[56]

network modifiers. All other atoms are treated as intermediates. While sharing oxygen atoms, network formers (> 335 kJ/mol), network modifiers (< 210 kJ/mol), and network intermediates (210 to 335 kJ/mol) attain different bond energies. The low bonding energy of the alkali atoms (i.e. network modifiers) in glass structure is an interesting aspect under the alkali environment, which influences the reaction rate of the material [49].

2.3 Morphological and Microstructural Characteristics

The scanning electronic microscope (SEM) image of WGP is shown in Fig. 4a. The glass particles are angular in shape with sharp edges and smooth surfaces [57]. Further, glass particles have less water absorption properties compared to other precursors [1, 42]. The X-ray diffraction (XRD) pattern of WGP, as shown in Fig. 4b, indicates a huge hump between 18° to 37°. It is due to the high amorphous phases in the WGP, which confirms a better reactivity of WGP [58].

2.4 Reaction Mechanism of WGP

The dissolution of glass in an aqueous solution was examined by El-Shamy and Pantano (1977) to understand its mechanism [59]. Under high pH values (> 9), the dissolution of glass takes place through ion exchange and silica network breakdown, whereas ion exchanges alone cause the dissolution of glass at lower pH values. In geopolymer materials, the presence of high alkali contents contributed to the breakdown of the silica network through nucleophilic attack

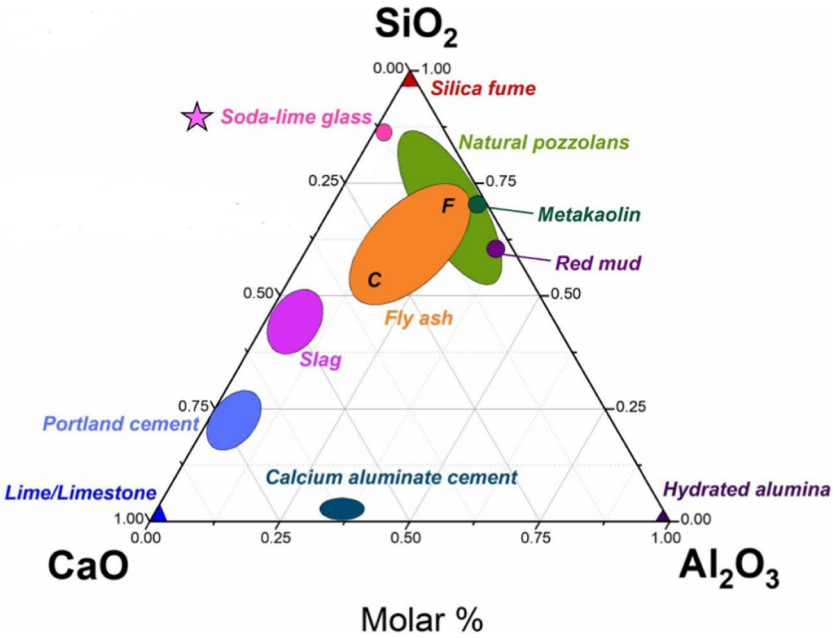

Fig. 2 Chemical compositions of soda lime glass and other commonly used cementitious materials [3]

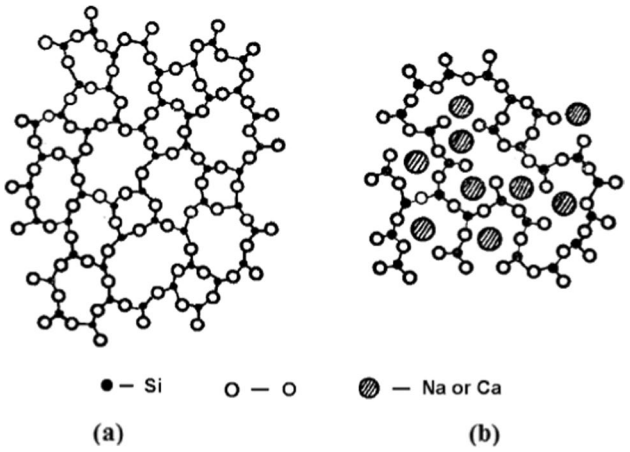

Fig. 3 Structure of **a** silicate glass and **b** Na-Ca silicate glass [50]

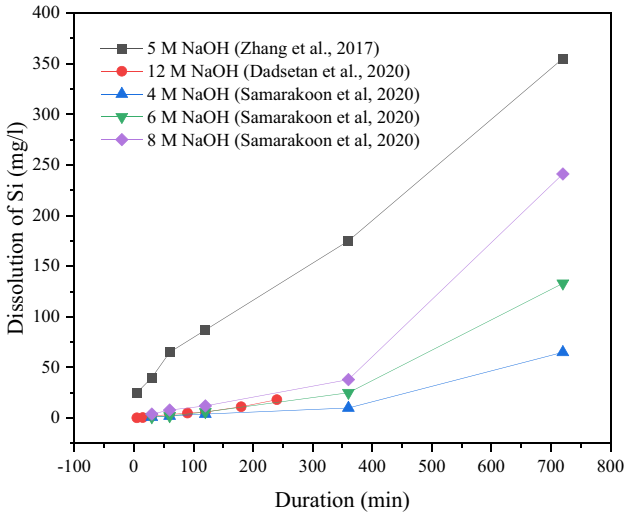

Fig. 5 Dissolution of silica (Si^{4+}) from WGP

of OH^- on silica tetrahedrons (Eqs. 1 and 2) [60]. Further, in the case of soda-lime glass, the Na-O bond has low bonding energy. Hence, earlier dissolution of sodium (Na^+) ions takes place through ion exchange (Eq. 3) [61]. It results in the rise of alkalinity of the pore solution and contributes to the better dissolution of silica in to pore solution. Thus, the incorporation of WGP as a precursor in geopolymer binders causes an abundance of reactive silica through ion exchange and silica network breakdown.

$$\equiv Si - O - Si \equiv + OH^- \rightarrow \equiv Si - OH + \equiv Si - O^- \quad (1)$$

$$\equiv Si - O^- + H_2O \rightarrow \equiv Si - OH + OH^- \quad (2)$$

$$\equiv Si - O - Na + H_2O \leftrightarrow \equiv Si - OH + Na^+OH^- \quad (3)$$

For quantitative analysis, different studies assessed the dissolution of silica (Si^{4+}) ions at different alkali concentrations and durations. The results of the literature studies are summarized in Fig. 5. For different alkali concentrations, the Si^{4+} ion dissolution increased with an increase in the duration [41, 42]. Further, it shows that the dissolution of ions increases with the increase in the alkali concentrations up to a certain extent (4 M to 8 M). However, the high viscosity of the alkali solution at higher concentrations reduces the mobility of ions from the solid precursors and causes low ionic dissolution. Hence, the ionic dissolution observed by Dadsetan et al. (2020) at 12 M NaOH concentration was lower compared to other studies [5]. These studies suggest that the moderate alkali concentration (4 M to 8 M) is favorable for better ionic dissolution. Moreover, it is important to note that the reactivity of WGP also depends on particle size, oxide compositions, temperature, etc.[62].

2.5 Heat of Hydration of WGP

Zhang et al. (2017) conducted an isothermal calorimetry analysis to study the heat of hydration of the alkali-activated WGP and compared it with alkali-activated slag and FA [41]. The result of the analysis (Fig. 6) showed two peaks for a given time period (up to 80 h). The first peak is related to the moisture and ionic dissolution from

Fig. 4 **a** SEM image and **b** XRD pattern of WGP

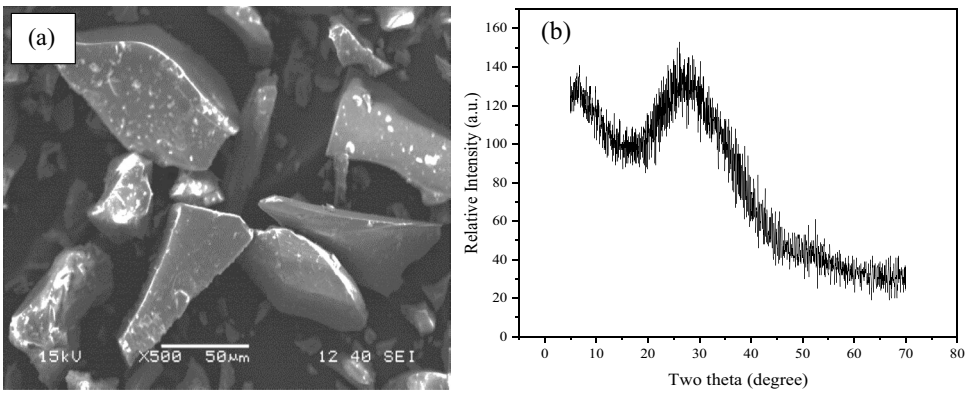

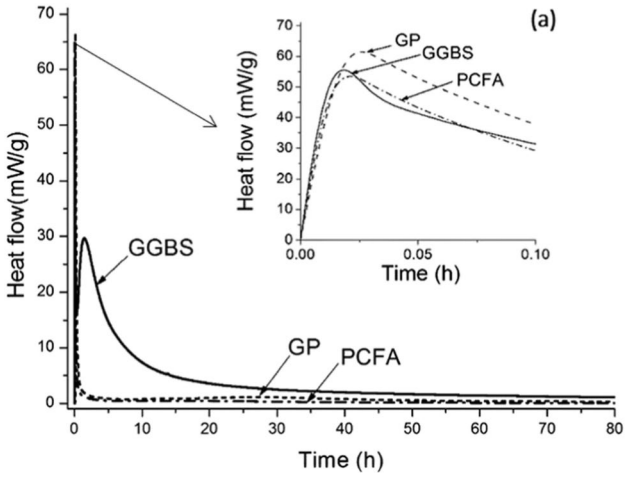

Fig. 6 Heat flow of WGP, slag and FA [41]. GP-glass powder; GGBS-granulated blast furnace slag; PCFA-powder coal FA

the materials, whereas the second peak is due to the geopolymer reactions between the dissolved ions. At initial periods, WGP has a higher peak curve compared to other precursors. As the reactivity of WGP is less compared to slag [40, 41, 51], the initial peak is mainly owed to the abundance of free water around the glass particles. Further, the second peak formed after prolonged duration confirms the slow and low reactivity of glass compared to slag. However, the reactivity of WGP was slightly higher compared to FA. The sequential order of reactivity of the materials is Slag > WGP > FA.

3 Fresh Properties

Fresh properties such as workability and setting time of the cementitious materials are prominent in understanding the ease of materials for practical application. Several literature studies examined the fresh properties of WGPG. The summary of these literature studies is presented in Table 3 and thoroughly discussed as follows.

3.1 Workability

Workability is important for assessing the ease of pumping and vibrating the concrete without segregation and bleeding effects [72]. The major parameters affecting the workability of the WGPG are the amount of WGP, the particle size of WGP, type and concentration of alkali activator and the liquid activator to solid binder (L/S) ratio. Hence, the below section reviews the influence of these parameters on workability.

3.1.1 Amount of WGP

The inclusion of WGP significantly influences the workability of the geopolymer materials. The study by Si et al. (2020) observed an increase in the workability by 8.46%, 12.17% and 21.16% with the inclusion of 5%, 10% and 20% of WGP in MK-WGP geopolymers [66]. Likewise, the majority of the literature studies, shown in Table 3, reported an enhancement in the workability of the geopolymer with the inclusion of WGP. The smooth surface and low water absorption properties of the glass particles are the main factors that contribute to an abundance of free water in the mix, which reduces inter-particle friction and increases workability [42, 65, 67]. In contrast, Lu and Poon (2018) observed a slight reduction in the workability of slag-FA geopolymers with the inclusion of WGP. It is due to the low specific surface area (SSA) of WGP and its large aspect ratios with uneven shape and sharp edges [69].

Additionally, the properties of the other precursors material used along with WGP also control the workability. The study of Manikandan et al. (2022) shows that the slag-WGP-10% MK (slump flow 170–198 mm) attains super workability compared to slag-WGP-10% FA (slump flow 117–162 mm) due to the low reactive silica of MK compared to FA [71]. Therefore, proper laboratory studies are required to assess the workability of the WGPG mixes for practical applications.

3.1.2 Particle Size of WGP

Lu et al. (2017) studied the flow behavior of the cement mortar with different particle sizes of WGP (204 µm, 88.5 µm, 47.9 µm and 28.3 µm mean diameter) [73]. The study reported that the workability of the mix improved with finer glass particles due to the reduction in inter-particle frictions caused by high aspect ratios of glass particles. Likewise, an analogous trend in geopolymer mixes with finer WGP is also feasible. However, such studies on the workability of geopolymer materials are hardly observed.

3.1.3 Type and Concentration of Alkali Activator

In general, alkali activation of precursor materials is carried out with different alkali solutions such as sodium hydroxide (NaOH), sodium silicate (Na_2SiO_3), potassium hydroxide (KOH), sodium carbonate (Na_2CO_3), etc. These solutions attain different viscosity affecting the workability of the mix. Wang et al. (2016) studied the workability of WGPG mix at varying proportions of NaOH and Na_2SiO_3 solutions (labelled as variations in alkali solutions in the original

Table 3 Summary of literature studies on fresh properties of WGPG

Precursor materials	WGP contents (wt. %)	Particle size of WGP	Alkali material and its concentration	L/S ratio	Remarks	Reference
Binary geopolymers						
Slag-WGP	10% and 20%	SSA[a]-4000 cm^2/g	NaOH-5 M NaOH-Na_2SiO_3 (0.5%, 0.75% and 1.00% of alkaline solution)	0.50, 0.55 and 0.60	Workability and setting time increased with increase in both WGP and L/S ratio. In addition, workability increases and setting time reduced with increase in alkaline solution	[51]
WGP-CAC[b]	76–100%	SSA-4500 cm^2/g	NaOH- Na_2SiO_3 with SiO_2/Na_2O ratio of 1.5	W/B ratio[c]- 0.485–0.555	Workability depends on type of CAC used. However, setting time is increased with rise in WGP	[63]
Slag-WGP	20% and 40%	SSA- 4000 cm^2/g	NaOH-5 M Na_2SiO_3 to NaOH ratio- 3.7, 6.03, 6.81 and 7.5	0.45, 0.50, 0.55 and 0.60	Workability and setting time increased with increase in both WGP and L/S ratio	[64]
FA-WGP	10–30%	D_{50}– 18.21 µm	NaOH-10 M Na_2SiO_3 to NaOH ratio-0.5	0.45	Workability increased and setting time reduced with increase in WGP	[1]
Slag-WGP	10–40%	MPS[d]- 25 µm	NaOH-12 M Na_2CO_3 to NaOH-1.5	W/B ratio-0.26	Workability increased with increase in WGP	[65]
MK-WGP	5–20%	D_{50}– 7.5 µm	NaOH-17.8 M Na_2SiO_3 to NaOH ratio-1.43	1.28	Workability and setting time increased with increase in WGP	[66]
WCC[e]-WGP	10–50%	Finer than 90 µm	NaOH-10 M Na_2SiO_3 to NaOH ratio- 2.5	0.20	Workability increased and setting time reduced with increase in WGP	[67]
Slag-WGP	10–40%	SSA- 4930 cm^2/g	NaOH-6 M	0.35	Setting time reduced with increase in WGP	[68]
Tertiary geopolymers						
Slag-WGP and Slag-FA-WGP	30%	SSA-1899 cm^2/g	NaOH-12 M	W/B ratio-0.40	Workability reduced with increase in WGP	[69]
30% to 50% Slag-30% to 50% FA-20% WGP	20%	D_{50}-10.2 µm	NaOH-8 M and Na_2CO_3 to NaOH-1.0	0.52	For NaOH, workability increased with WGP, whereas, workability is inconsistent with inclusion of Na_2CO_3. Different mix proportions showed different setting times	[56]
Slag-WGP-CAC	10–70%	D_{50}-16.36 µm	Na_2SiO_3 with SiO_2/Na_2O ratio of 2.11	0.13	Workability and setting time increased with increase in WGP	[70]
FA-WGP-50% slag		D_{50}-11.5 µm	NaOH- 8 M	0.40, 0.45 and 0.50	Workability and setting time increased with increase in WGP and L/S ratio	[42]

Table 3 (continued)

Precursor materials	WGP contents (wt. %)	Particle size of WGP	Alkali material and its concentration	L/S ratio	Remarks	Reference
Slag-WGP-10% FA and Slag-WGP-10% MK	25–40%	< 75 µm	NaOH-8 M Na_2SiO_3 to NaOH ratio- 2.5	0.55	Workability increased with increase in WGP. However, workability of Slag-WGP-10% MK is higher than that of Slag-WGP-10% FA	[71]

[a]SSA-Specific surface area;
[b]CAC-Calcium aluminate cement;
[c]W/B ratio-Water to binder ratio;
[d]MPS-Mean particle size;
[e]WCC-Waste cement concrete

article) [51]. The study reported that the low proportions of Na_2SiO_3 solution are beneficial for better workability of the mix. It is ascribed to the high viscous behavior of the Na_2SiO_3 solution compared to the NaOH solution. In addition, different concentrations of the alkali activator show different viscosities and influence the workability. Literature studies on conventional geopolymer materials showed that the viscosity of the geopolymer mix increases with an increase in the alkali concentration and hence, reduces the workability [74]. Moreover, at higher concentrations, the quick ionic dissolution from precursors further renders the workability with higher viscosity. Although several literature studies used high alkali concentrations for WGPG (Table 3), the surface properties of the WGP aid in preserving the workability [1, 65–67, 69].

3.1.4 L/S Ratio

The L/S ratio is another main parameter influencing the workability of WGPG paste. Wang et al. (2017) reported that the workability of slag-40%WGP geopolymer increased by 20.0% and 33.33% with an increase in 0.05 and 0.10 L/S ratio [64]. A similar trend in workability with an increase in the L/S ratio was also observed in other literature studies, as shown in Table 3 [42, 51]. Higher L/S ratios allow more liquid in the fresh mix for lubrication, improving workability.

3.2 Setting Time

Setting time of cementitious materials is essential for managing transportation, placement and compaction of concrete, and removal of shuttering in the field. As setting time is highly dependent on the reaction phases, the parameters governing the formation of reaction phases also control the setting time. Hence, in this section, the effect of parameters such as the amount of WGP, its particle size, type and concentration of alkali activator and L/S ratio on the setting time of WGPG are thoroughly reviewed.

3.2.1 Amount of WGP

As discussed in Section 2.4, the reaction mechanism of WGP predominantly influences the phase formations and associated setting time. As shown in Table 3 and Fig. 7, several studies reported an increase in the setting time for both binary and tertiary geopolymer mix with the inclusion of WGP [42, 64, 66, 71]. Li et al. (2020) observed an initial setting time of 48 min, 52 min, 60 min and 90 min, and a final setting time of 55 min, 58 min, 68 min and 108 min with the inclusion of 10%, 30%, 50% and 70% of WGP in slag-WGP- calcium alumina cement (CAC) mixes. The surface properties of the glass particle, which avails free water in the mix, are the main considerations for a prolonged setting

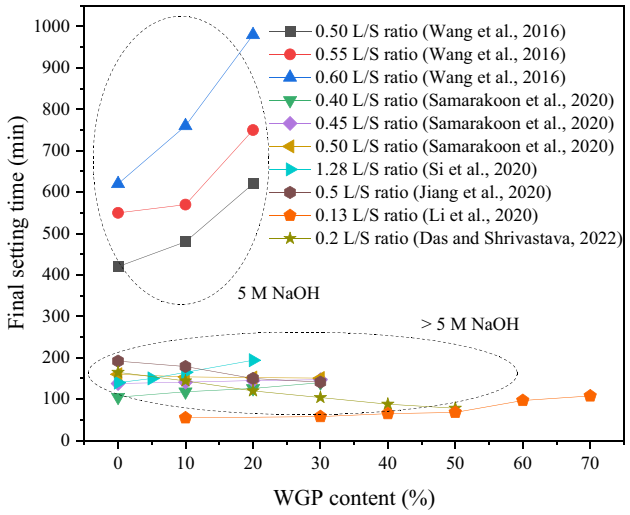

Fig. 7 Final setting time of WGPG

time. Further, few studies reported that the low reactive of the WGP, compared to co-precursors (slag/MK), also causes the slow setting of the geopolymer mix [42, 51]. In contrast, few other studies reported early setting with WGP due to the higher reactivity of WGP compared to FA/WCC [1, 67]. However, Varma and Singh (2023) observed a slightly earlier setting in the slag-WGP mix with WGP inclusion [68]. It was argued that the dissolution of alkali cation (Na^+) from WGP increases the overall alkalinity of the slag-WGP mix, and results in an earlier setting with faster geopolymer. Moreover, Liu et al. (2019) observed contradictory setting times in a tertiary geopolymer (slag-FA-20% WGP) due to different mix proportions of slag and FA content [56]. These studies show that the setting time of WGPG depends not only on the properties of WGP but also on the properties of co-precursors.

3.2.2 Type and Concentration of Alkali Activator

The setting time of geopolymer pastes is significantly varied with the type of alkali activator and its concentration. Liu et al. (2019) prepared WGPG with 8 M NaOH and 8 M NaOH-Na_2CO_3 solution and observed an earlier setting with NaOH solution (by 144 to 231 min for the initial setting and 216 to 271 min for the final setting). Similarly, Wang et al. (2016) observed an earlier setting with an increase in the NaOH content in a WGPG prepared with NaOH-Na_2SiO_3 solution [51]. These studies indicate that the NaOH solution shortens the setting time compared to other alkali solutions.

In addition, the concentration of NaOH solution also affects the setting behaviour of the WGP-geopolymer. As shown in Fig. 7, Wang et al. (2016) reported a final setting time of 420 min to 980 min with 5 M NaOH concentration, whereas several other studies reported an earlier setting of about 50 min to 200 min with higher NaOH concentration (8 M to 18 M). An increase in alkali concentration causes rapid development of reaction phases due to the augmentation of ionic dissolution from precursors, as discussed in Section 2.4. This results in the earlier setting of the geopolymer mix at higher concentrations.

3.2.3 L/S Ratio

For geopolymer material, the quantity of alkali solutions always plays a significant role and affects the setting times. With increased L/S ratios, the setting time of the WGPG mixes is significantly increased (Fig. 7). As the L/S ratio increases, the availability of free water in the mix increases and delays the setting of the material [42, 51, 64]. In addition, Samarakoon et al. (2020) observed that the influence of WGP content on setting time was reduced at higher L/S ratios due to the difference in the physical properties of the WGP and other co-precursors used in the study [42].

3.2.4 Mixing Time

The setting period of geopolymer paste is affected by the mixing time. In general, an increase in mixing time increases the setting time of geopolymer paste [75]. However, as per the author's knowledge, the studies showing the effect of mixing time on the setting of WGPG are hardly identified. As the surface properties of glass differ from the other materials, it is essential to assess the mixing time effect on the WGPG.

4 Hardened Properties

4.1 Mechanical Strength

The strength of the WGPG binders is mainly controlled by the synthesis parameters (amount of WGP, the particle size of WGP, type of alkali activator and its concentration, and L/S ratio) and its curing environment. Hence, the effect of these parameters on the strength properties of the WGPG is reviewed and discussed below.

4.1.1 Amount of WGP

The incorporation of silica-rich WGP in the synthesis of geopolymer materials causes a significant change in the strength properties. The variation in the 28-day compressive strength (f_c), flexural strength (f_f) and tensile strength (f_t) of the geopolymers at different WGP contents is presented in Fig. 8 and Table 4. Several studies showed the strength improvement with the inclusion of WGP up to a certain level of replacement (5% to 30%) in both binary and tertiary

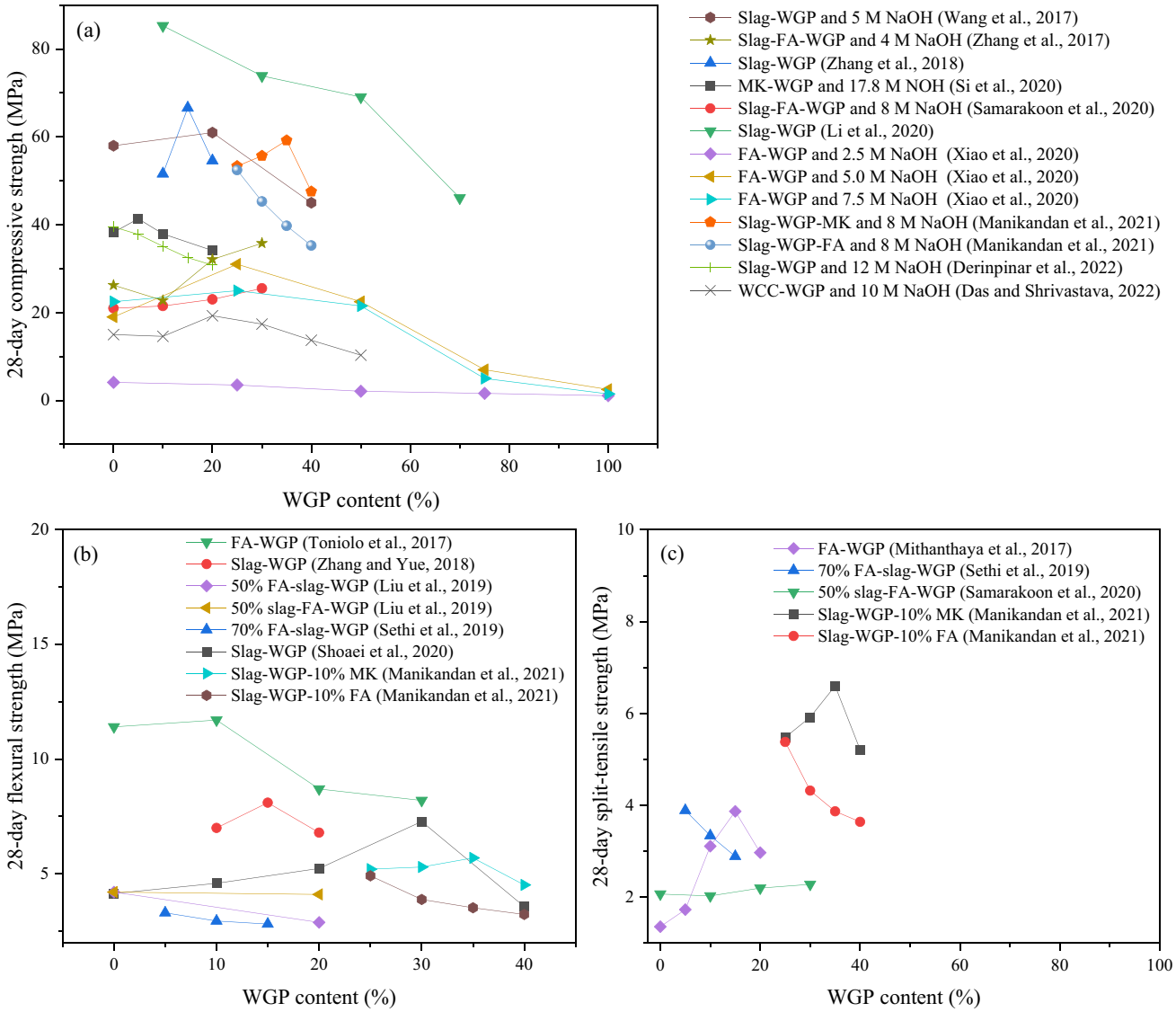

Fig. 8 Strength properties of WGPG at varying WGP contents. **a** Compressive strength, **b** flexural strength and **c** tensile strength

geopolymer systems. Samarakoon et al. (2020) observed a maximum f_c and f_t at 30% of WGP in slag-FA-WGP mixes [42]. For FA-WGP mixes, Xiao et al. (2020) observed a maximum f_c at 25% of WGP [13], whereas Si et al. (2020) observed a peak f_c at 5% of WGP in MK-WGP mix [66]. The strength enhancement in these WGPG mixes is mainly ascribed to the availability of reactive silica from WGP, contributing to an acceleration in the geopolymer mechanism and the formation of stronger Si-O-Si bonds [66, 71]. Further, the aluminosilicate phases, such as calcium silicate hydrate (C-S-H), calcium alumina silicate hydrate (C-A-S-H), and sodium alumina silicate hydrate (N-A-S-H) are the primary reaction phases that occur in WGPG [4, 41, 42].

In contrast, other research studies showed a negative impact of WGP on mechanical strength. Li et al. (2020) and Derinpinar et al. (2022) observed a continuous strength decrease (f_c) in the slag-WGP with the inclusion of WGP due to the low reactivity of WGP compared to slag [70, 80]. Bobirica et al. (2015) reported a decrease in the 28-day f_c of FA-WGP and FA-slag-WGP geopolymers cured at 60° C for 24 h [52]. The rise in Si/Al ratio due to enormous Si^{4+} ion dissolution from the WGP was reported as the primary basis for strength loss. As literature studies show contradictory results, the prediction of mechanical strength with literature studies is erroneous and needs a though laboratory investigation before its practical application.

Table 4 Summary of literature studies on strength properties of WGPG

Precursor materials	Particle size of WGP	Alkali material	L/S ratios	Specimen size (mm)	Curing environment	Optimum WGP (%)	Maximum 28-day strength	Reference
Binary geopolymers								
Slag-WGP	SSA[a]-4000 cm^2/g	5 M NaOH-Na_2SiO_3	0.50, 0.55 and 0.60	50×50×50	20 °C	20%	f_c[b]-55 MPa at 0.55 L/S ratio	[51]
Slag-WGP FA-WGP	MPS[c]-23 µm	5 M NaOH-Na_2SiO_3	0.44	50×50×50	60 °C steam curing	30%	f_c-78 MPa	[40]
FA-WGP	< 600 µm	8 M NaOH	Not specified	150×150×150 150×300	Not specified	15%	f_c-22.60 MPa f_t[d]-3.87 MPa	[76]
FA-WGP	< 60 µm	8 M NaOH-Na_2SiO_3	0.40	14×31.5	60 °C for 24 h	-	Both f_c and f_f[e] are reduced	[77]
Slag-WGP	SSA-4000 cm^2/g	5 M NaOH-Na_2SiO_3	0.45, 0.50, 0.55 and 0.60	50×50×50	Room temperature	20%	f_c-67 MPa at 0.50 L/S ratio	[64]
FA-WGP	MPS < 23 µm	5 M, 8 M and 10 M NaOH	0.45	Not specified	60 °C for 48 h	36%	f_c-48 MPa	[78]
Slag-WGP	SSA- 5000 cm^2/g	NaOH-Na_2SiO_3	W/B ratio[f]-0.40	40×40×160	20 °C	15%	f_c-66.66 MPa and f_f—8.1 MPa	[7]
MK-WGP	SSA- 3820 cm^2/g	12 M NaOH-Na_2SiO_3	0.45 to 0.70	50×50×50	Ambient temperature	25%	f_c-55 MPa	[5]
FA-WGP	D_{50}-18.21 µm	17.8 M NaOH-Na_2SiO_3	0.45	25×50	60 °C ± 2 for 24 h	25%	f_c-53.22 MPa	[1]
Slag-WGP	D_{50}-16.36 µm	Na_2SiO_3	0.15	40×40×40	23 ± 5 °C and RH[g] > 60 ± 10%	-	Reduces	[70]
Slag-WGP	MPS-25 µm	12 M NaOH-Na_2SiO_3	0.38	50×50×50 160×40×40	Not specified	30%	f_c-53.2 MPa, f_f-7.28 MPa	[65]
MK-slag	MPS-7.5 µm	17.8 M NaOH-Na_2SiO_3	1.28	50×50×50	23 °C	5%	f_c-41.36 MPa	[66]
Slag-WGP and FA-WGP	D_{50}-41.9 µm, 159.1 µm and 302.1 µm	2.5 M KOH-Na_2SiO_3	0.50	25×50	20 °C, 50 °C, 80° C and 100 °C for 24 h	50%	f_c-46.5 MPa in slag-WGP at 80° C and 17.25 MPa in FA-WGP at 100° C	[4]
FA-WGP	SSA- 3620 cm^2/g	NaOH	W/B ratio-0.5	40×40×40	20 ± 2 °C and RH > 95%	-	Reduces	[54]
Slag-WGP	MPS-10.38 µm	4 M NaOH-Na_2SiO_3	W/B ratio-0.35	50×50×50	Not specified	50%	f_c- 65.5 MPa	[79]
WCC[h]-WGP	D_{50}-12.84 µm	10 M NaOH-Na_2SiO_3	0.20	50×50×50	30 °C and 85% RH	25%	f_c-19.3 MPa	[67]
Slag-WGP	SSA-2944 cm^2/g	12 M NaOH	Not specified	50×50×50 100×200	Room temperature	-	Reduces	[80]
Slag-WGP	SSA-11450 cm^2/g	6 M NaOH	0.35	50×50×50	60 °C for 24 h	10%	f_c-42.7 MPa	[68]

Table 4 (continued)

Precursor materials	Particle size of WGP	Alkali material	L/S ratios	Specimen size (mm)	Curing environment	Optimum WGP (%)	Maximum 28-day strength	Reference
Tertiary geopolymers								
FA-WGP and FA-WGP-20% slag	< 75 µm	NaOH-Na_2SiO_3	Not specified	50 × 100	60 °C for 24 h	-	Reduces	[52]
50% Slag-FA-WGP	D_{50}-5.07 µm	4 M NaOH	0.42	40 × 40 × 160	20 °C and RH > 98%	30%	f_c-35.8 MPa	[41]
Slag-FA-30% WGP	SSA-1899 cm^2/g	10 M NaOH	W/B ratio-0.40	50 × 50 × 50	25 ± 2 °C and RH 50 ± 5%	-	Reduces	[69]
50% Slag-FA-WGP	SSA-9900 cm^2/g	NaOH-Na_2CO_3	0.52	40 × 40 × 160	20 °C	-	Both f_f and f_f are reduced	[56]
70% FA-slag-WGP	10–600 µm	4 M, 8 M and 12 M NaOH	Not specified	150 × 150 × 150 150 × 300	60 °C for 48 h	-	Both f_f and f_f are reduced	[81]
50% Slag-FA-WGP	D_{50}-11.5 µm	8 M NaOH	0.40	38 × 76	23 °C, wet curing and 60 °C for 24 h	30%	f_c-34.5 MPa under wet curing	[42]
Slag-WGP-10% MK and Slag-WGP-10% FA	< 75 µm	8 M NaOH-Na_2SiO_3	0.55	150 × 150 × 150 200 × 100 500 × 100 × 100	Not specified	35% in Slag-WGP-10% MK	For slag-WGP-10% MK, f_c-59.21 MPa, f_t^i-6.6 MPa and f_f-5.7 MPa. However, strength properties reduce in Slag-WGP-10% FA	[71]

[a]SSA-Specific surface area;

[b]f_c-compressive strength;

[c]MPS-Mean particle size;

[d]f_t-tensile strength;

[e]f_f-flexural strength;

[f]W/B ratio-water to binder ratio;

[g]RH-Relative humidity;

[h]WCC-Waste cement concrete

4.1.2 Particle Size of WGP

The particle size of the WGP highly influences the pozzolanic nature and corresponding strength properties [3]. Zhang et al. (2020) used three different sizes of WGP with D_{50} of 41.9 µm, 159.1 µm and 302.1 µm for synthesis of slag-WGP and FA-WGP geopolymers [4]. For slag-WGP geopolymers (80 °C for 24 h), the peak 28-day f_c reduced by 16.55% and 61.72% when the increase particle size increased from 41.9 µm to 159.1 µm and 302.1 µm, respectively. In the case of FA-WGP geopolymer cured at 100 °C for 24 h, the peak 28-day f_c reduced by 47.82% and 55.07%, respectively. The WGP with finer particle size contributes to higher dissolution under an alkali medium and enhances the formation of better silica-alumina geopolymer gel. To utilize this advantage, most researchers used fine WGP by considering 75 µm as the threshold particle size, as shown in Table 4 [3].

4.1.3 Type of Alkali Activator and its Concentration

As shown in Table 4, several researchers activated WGPG using NaOH, KOH, Na_2SiO_3, Na_2CO_3, and their blends. Wang et al. (2016) synthesized slag-WGP geopolymer using NaOH-Na_2SiO_3 solution and observed an increase in the f_c with a rise in NaOH solution content [51]. As WGP contributes a significant amount of Si^{4+} ions, the use of commercial silicates (Na_2SiO_3) further raises the Si^{4+} ions in the mix and causes strength reduction due to the deficiency of Al^{3+} ions [5, 42]. This phenomenon is also supported by studies conducted on WGP-based alkali solutions [46, 48]. Thus, the use of commercial silicates can be reduced in WGPG. Further, the study of Liu et al. (2019) reported a high f_c and f_f due to a better formation of C-S–H phases in slag-FA-WGP geopolymers prepared with NaOH-Na_2CO_3 solution compared to NaOH solution [56]. Dadsetan et al. (2020) studied the effect of Na_2O/SiO_2 ratio (0.22, 0.24, 0.26, and 0.28) by varying the NaOH and Na_2SiO_3 solution contents in MK-WGPG [5]. It was reported that, at optimum WGP content (25%), a rise in Na_2O/SiO_2 ratio significantly reduces the f_c of the material due to the free Na^+ ions in the matrix, which causes efflorescence. These studies clearly indicate that the strength of the geopolymer significantly depends on the type of activator.

In addition, the concentration of alkali activator also causes prominent changes in the strength properties of WGPG (Fig. 8). Xiao et al. (2020) activated the FA-WGP geopolymer with varying NaOH concentrations (2.5 M, 5.0 M, 7.5 M and 10 M) and observed a maximum f_c at 5 M NaOH concentration [13]. Similarly, Toniolo et al. (2018) observed a high 28-day f_c of FA-WGP geopolymer at 8 M NaOH concentration compared to 5 M and 10 M NaOH concentrations [78]. In NaOH solution, OH^- acts as a catalysis promoting the dissolution of Si^{4+} and Al^{3+} ions, and the Na^+ ion balances the deficiency of ions around alumina tetrahedrons [74]. Hence, strength properties improved with an increase in the alkali concentration. However, at higher concentrations, excess Na^+ ions alter the Na_2O/SiO_2 ratio and reduce the strength. Considering the effect of alkali concentration, several studies synthesized WGPG with optimal concentrations of NaOH (4–8 M) and reported a fair strength gain [41, 51, 64, 68].

4.1.4 L/S Ratio

The quantity of alkali solution controls the ionic dissolution from raw material, therefore, influences the strength development. Wang et al. (2016) synthesized slag-WGP geopolymers at varying L/S ratios (0.50, 0.55 and 0.60) and reported a higher strength at 0.55 L/S ratio [51]. In another study, Wang et al. (2017) observed a higher strength at 0.50 L/S ratio when slag-WGP geopolymers are produced with varying L/S ratios of 0.45, 0.50, 0.55 and 0.60 [64]. As the L/S ratio increases, more Si^{4+} and Al^{3+} ions get dissolved from the precursors and develop strong geopolymer networks. However, beyond a threshold L/S ratio, high initial water content embeds voids in the hardened material and disturbs the structural integrity resulting in strength loss [74]. Further, the presence of high Na^+ ions at higher L/S ratios also causes strength reduction. Thus, based on the literature studies (Table 4), the threshold L/S ratio for WGPG is observed to be in the range of 0.40 to 0.55.

4.1.5 Curing Environment

The curing environment is one of the crucial aspects influencing the geopolymer mechanism [82–84]. It includes both the curing period and curing temperature. Under ambient conditions, the strength of the WGPG enhances with an increase in the curing period [5, 7]. In slag-FA-WGP geopolymer, Samarakoon et al. (2020) observed peak f_c at 20% WGP for 7-day curing and at 30% WGP for 28-day curing [42]. However, few other studies reported significant strength improvement only after a prolonged curing period of 14 days [13, 51]. It is mainly due to the low reaction mechanism of WGP at ambient temperature, hence, requiring prolonged curing periods.

For enhancing the reactivity of the WGP, the majority of the literature studies, as shown in Table 4, used the initial heat-curing technique. Zhang et al. (2020) prepared slag-WGP and FA-WGP geopolymers by exposing specimens to different temperatures (20 °C, 50 °C, 80 °C and 100 °C) for an initial 24 h [4]. The study observed peak strength at 80 °C for slag-WGP (46.5 MPa) and 100 °C for FA-WGP (17 MPa). It showed that the reactivity of WGP significantly escalated at elevated temperatures contributing to strength

enhancement. In addition, several other studies used 60 °C (24 h to 48 h) to achieve better mechanical strength properties for WGPG [1, 42, 52, 68, 85]. Conversely, the study of Martinez-Lopez and Escalante-Garcia (2016) reported a strength reduction in slag-WGP geopolymer cured at 60 °C and 70 °C [86]. The contraction of silica-based gels at initial curing periods due to the evaporation of unbounded water from the gel networks is considered as a reason for strength reduction at high temperatures.

Samarkoon et al. (2020) examined the effect of ambient, wet, and initial heat curing (60 °C for 24 h) techniques on the f_c of slag-FA-WGP geopolymers [42]. The study reported that the heat curing techniques attain high early strength (30.0–32.0 MPa at 7-day curing). However, at longer curing periods, the strength improvement is trivial with the heat curing technique due to low moisture content in the system, which retards the longer poly-condensations. In addition, wet curing technique attain superior strength (41.5–50.0 MPa) at 56-day prolonged curing due to the continuous availability of moisture for hydration reactions. Moreover, Maraghechi et al. (2017) used 56-day prolonged steam curing (60 °C) technique and observed peak strengths for slag-30% WGP (86.0 MPa) and FA-20% WGP (62.0 MPa) [40].

5 Durability of WGPG

5.1 Alkali-Silica Reactions (ASR)

In general, geopolymer materials may induce ASR due to the presence of high alkali contents in the pore solution with high calcium components [87]. As WGP has high silica components with fair calcium components (10–13%), it is highly susceptible to ASR. Several literature studies examined the ASR expansion of WGPG following ASTM C1260, and the results are shown in Fig. 9. Maraghechi et al. (2017) conducted the ASR expansion of slag-WGP and FA-WGP geopolymers [40]. The study observed a decline in the ASR expansion of the slag-based geopolymer mix and an increase in the ASR expansion of FA-based geopolymer with the incorporation of WGP. Further, the study of Shoaei et al. (2020) reported a slight expansion of slag-based geopolymer with WGP [65]. Nevertheless, both these studies showed that the expansion of WGPG is within the permissible limit as per ASTM C1260 (< 0.10%). In contrast, He et al. (2020) observed a severe ASR expansion in slag-WGP geopolymers. It is further considerably reduced, lower than OPC, with the usage of CAC [88, 89]. Moreover, several researchers considered that the ASTM C1260 might not be an appropriate method to measure ASR in geopolymer materials due to the short duration of the test, high-temperature exposure and strong external alkali solution (1 M NaOH) [87]. Further, the loss of alkali content from pore solution, when immersed in water for an initial 24 h after demolding, also dilutes the ASR reactions [3]. Hence, proper testing methodology should be for assessing the ASR reactions of WGPG.

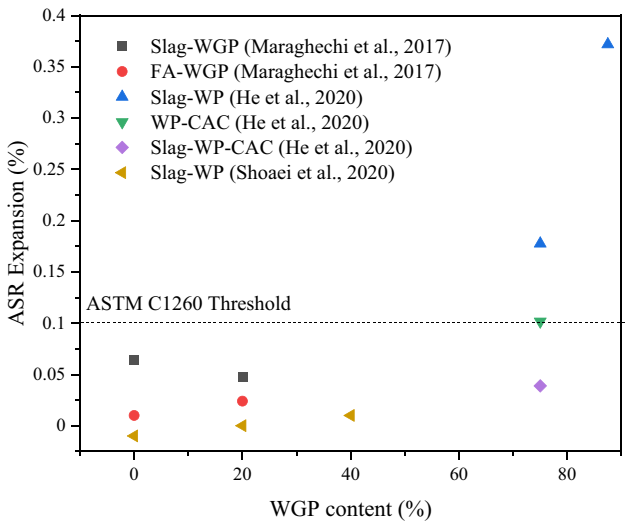

Fig. 9 ASR expansion (14-day) of WGPG as per ASTM C1260

5.2 High-Temperature Exposer

In general, geopolymer materials have high resistance to fire accidents compared to OPC [29, 90]. However, water evaporation and swelling of unreacted silica occur in geopolymer structures at high-temperature exposure, causing shrinkage cracks and strength reduction [91]. Jiang et al. (2020) assessed the strength of FA-WGP geopolymer by exposing it to high temperatures (800 °C, 1000 °C and 1200 °C) for 2 h. For 20% WGP, the strength was reduced from 53.33 MPa to 24.48 MPa, 13.87 MPa and 2.13 MPa when exposed to 800 °C, 1000 °C and 1200 °C, respectively. However, the strength of FA geopolymer (without WGP) was reduced from 50 MPa to 18.5 MPa, 8.5 MPa and 1.5 MPa, respectively. The higher residual strength of FA-WGP geopolymers after exposure to 800 °C and 1000 °C is related to the melting of glass (melting point-700 °C) into surrounding pore structure which causes denser structure formations [1]. However, no such filling activities were observed at 1200 °C. Similarly, Derinpinar et al. (2022) examined the residual strength of the slag-WGP geopolymer by subjecting to 150 °C, 300 °C, 450 °C, 600 °C and 750 °C for 1 h [80]. At 750 °C, the f_c was reduced by 61.99%, 60.75%, 58.92%, 57.00% and 55.49% with the inclusion of 0%, 5%, 10%, 15% and 20% of WGP. Thus, the rate of strength loss was controlled with WGP. These studies showed that the WGPG has fair resistance towards high-temperature exposures.

5.3 Chemical Attacks

It is quite often that the concrete structures in industrial areas, sewer pipes, and wastewater sewage networks are subject to chemical environments and deteriorate. Hence, it is essential to study the effect of the chemical environment on new binding materials. Wang et al. (2017) exposed the slag-WGP geopolymer to 24 h drying followed by 24 h sulfate immersion up to five cycles and observed a decrease in weight loss with the inclusion of WGP [64]. After the fifth cycle, the weight loss percentage decreased from 3.5% to 3.2% and 2.6%, with 10% and 20% of WGP, respectively. Further, Zhang et al. (2018) immersed slag-WGP geopolymer specimens in 5 wt% Na_2SO_4 and 5 wt% $MgSO_4$ for up to 90 days. The study reported a decline in strength loss by 1.9–3.6% with the incorporation of WGP [7]. However, the strength loss in the $MgSO_4$ solution is higher than Na_2SO_4 solution due to the superior decalcification effect of Mg^{2+} ions compared to Na^+ ions. Recently, Das and Shrivastava (2022) investigated the durability of WCC-WGP geopolymers under acidic (5% H_2SO_4 and 5% HCl) and sulfate (10% $MgSO_4$) solutions for 120 days [67]. The long-term durability studies showed that WGP enhanced the durability of the WCC geopolymers under both acidic and sulfate attacks.

5.4 Drying Shrinkage

In general, shrinkage occurs in geopolymer material through capillary stress, disjoining pressure and chemical interaction, which disturbs the structural integrity [27]. Zhang and Yue (2018) examined the drying shrinkage of OPC, slag geopolymers and slag-WGP geopolymers [7]. The study reported a significant reduction in the drying shrinkage (20.3%) of slag geopolymer with the inclusion of 14.57% of WGP. However, the slag-WGP geopolymer has higher shrinkage in comparison to OPC. Conversely, few studies reported higher drying shrinkage with the addition of WGP due to reduced strength and increased mesopores [56, 88]. Nevertheless, Xiao et al. (2021) observed a significant reduction in drying shrinkage of WGP geopolymer, lower than OPC, with the addition of calcium sulfoaluminate cement (> 50%) [92]. These literature studies disclose that the shrinkage behavior of geopolymer materials is complex and depends on various parameters, such as the chemical composition of precursors, type and concentration of alkali activators, and curing temperature. Hence, systematic laboratory studies are required prior to a mix design for field applications.

5.5 Carbonation

The atmospheric CO_2 interacts with geopolymer along its surface and causes significant changes in the reaction phase. Hence, the resistance of geopolymer material against carbonation is an essential durability property. Liu et al. (2019) studied the carbonation resistance of slag-FA-WGP geopolymers by exposing to CO_2 at 20% of constant ambient pressure. The results indicated that the incorporation of WGP improved the resistance of the slag-FA mixes. However, the carbonation resistance was prominent in NaOH-activated slag-FA-WGP mixes compared to NaOH-Na_2CO_3.

6 Leachate Analysis

Table 5 summarizes the leaching of heavy metal ions from various WGPG. In the study of Toniolo et al. (2018), the leaching of Cr was significantly reduced from 0.467 mg/l (raw FA) to a range of 0.0052–0.0101 mg/l (FA-WGP geopolymer matrix). In another study, Bobirică et al. (2018) observed a noteworthy decline in the leaching of Hg from 35.95 mg/l (raw WGP) to a range of 1.25–6.11 mg/l (FA-WGP and FA-WGP-20% slag geopolymer matrix). Further, these studies considered WGPG as non-hazardous material based on the standards specification such as European Standard for waste toxicity evaluation (EN 12457–2) and Universal Treatment Standards (40 CFR 268.48). Thus, WGP can be used as a valuable precursor material for geopolymers without compromising encapsulation behavior.

7 Sustainability Analysis

Although WGPG attains significant mechanical and durability properties, sustainability studies are essential for large-scale applications. Shoaei et al. (2020) observed that the embodied energy (E-energy) and the embodied CO_2 (E-CO_2) of the slag-WGP mortar were slightly reduced with the incorporation of WGP [65]. At 40% of WGP, the E-energy and E-CO_2 were reduced by 6.74% and 5.20%, respectively. It is due to the low environmental impact of WGP (E-energy-0.52 MJ/kg and E-CO_2-0.043 kg CO_2/kg) compared to slag (E-energy-1.07 MJ/kg and E-CO_2-0.09 kg CO_2/kg). Nevertheless, the study of Xiao et al. (2020) showed an increase in the E-energy and E-CO_2 of the FA-based geopolymers with the dosage of WGP owing to the higher environmental impact of WGP (E-energy-0.76 MJ/kg and E-CO_2-0.05 kg CO_2/kg) compared to FA (E-energy-0.10 MJ/kg and E-CO_2-0.004 kg CO_2/kg) [13]. In addition, alkali activators used in WGPG are the main components responsible for a majority share of environmental impact (30–40%). Although different WGPG showed dissimilar trends in environmental impact, the overall E-energy and embodied CO_2 (E- CO_2) of the WGPG is much lower than that of OPC (Fig. 10). Hence, the synthesis of WGPG aids in the development of eco-friendly binders.

Table 5 Leaching of heavy metal ions from WGPG

Precursor materials	Optimum WGP (%)	Leaching of heavy metal ions (mg/l)									Reference
		As	Cd	Cr	Cu	Pb	Se	Zn	Hg	Ni	
FA	NA[a]	< 0.049	< 0.002	0.467	0.028	< 0.047	0.022	< 0.2	-	-	[78]
WGP	NA	< 0.049	0.001	0.043	0.036	0.018	0.018	0.088	-	-	
FA-WGP	24	1.177	0.003	0.0101	0.111	0.07	0.039	< 0.203	-	-	
	36	0.134	0.004	0.0101	0.115	0.078	0.048	< 0.203	-	-	
	46	0.147	0.008	0.0052	0.197	0.117	0.048	< 0.203	-	-	
Inert material	NA	0.50	0.04	0.50	2.00	0.50	0.10	4.00	-	-	
Non-hazardous material[b,c]	NA	2.00	1.00	10.00	50.00	10.00	0.05	50.0	-	-	
WGP		1.23	0.06	4.48	207.53	44.90	-	101.71	35.95	16.43	[93]
FA		102.30	2.13	4.33	279.04	258.30	-	1785.12	ND[d]	7.00	
Slag		41.26	0.04	0.06	12.26	6.01	-	1235.33	ND	0.11	
FA-WGP	0	264.40	0.07	5.57	317.25	ND	-	0.14	ND	3.09	
	10	300.20	0.05	3.75	340.08	0.07	-	0.57	ND	1.92	
	20	403.62	0.06	2.87	301.81	0.17	-	0.25	1.61	1.38	
	30	320.37	0.04	1.41	336.08	3.21	-	1.23	6.11	1.63	
FA-WGP-20% slag	0	191.78	0.08	5.51	268.84	2.00	-	9.02	ND	3.40	
	10	223.37	0.10	4.94	226.82	24.70	-	13.87	1.25	4.90	
	20	224.22	0.09	5.58	172.80	39.15	-	11.54	1.26	3.56	
	30	179.89	0.07	4.53	134.76	52.43	-	5.36	1.47	2.83	
UTS[b, e]	NA	500	0.11	0.60	-	0.75	-	4.30	0.025	11.00	

[a]NA-Not applicable;

[b]Threshold limits;

[c]European Standard for waste toxicity evaluation (EN 12457);

[d]ND-Not detected;

[e]UTS-Universal Treatment Standards list (Code of Federal Regulations)

8 Conclusions and Perceptions

8.1 Conclusions

Based on the typical review of WGPG following conclusions are drawn out:

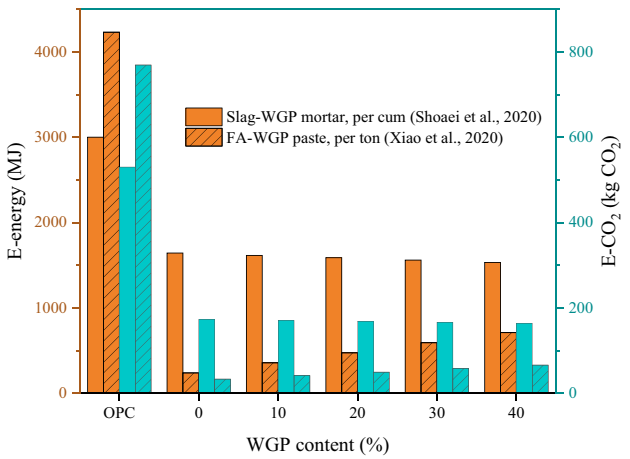

Fig. 10 E-energy and E-CO_2 of WGPG

- The chemical composition of waste glass, obtained from various sources, is mainly composed of silica, calcium and sodium oxides. Hence, waste glass procured from different sources can be significantly used as a precursor for geopolymers.
- The smooth surface and low water absorption properties of the glass particles enhance the workability and setting time of the geopolymer mix. In addition, the particle size of the WGP, type of co-precursors and alkali concentration also causes noteworthy changes in the fresh properties.
- The incorporation of WGP up to a certain replacement level (5–30%) improves the long-term mechanical properties of the geopolymers with the formation of strong Si–O-Si bonds. However, the slow reactivity of WGP negatively impacts the earlier strength gain. Further, an appropriate alkali concentration (4–8 M) in the WGPG exhibits significant properties.
- As per ASTM C1260, the escalation in ASR expansions of WGPG is within the permissible limits but higher than that of OPC. Moreover, the use of CAC can further reduce ASR expansions in WGPG.
- Under high-temperature exposures (> 700 °C), a denser microstructure was developed in WGPG due to the melt-

ing of WGP into surrounded pore structure and retained the residual strength. Further, the use of WGP enhances the resistance of geopolymer against chemical attacks (acid and sulfate) and drying shrinkage.

- A three-dimensional framework developed in WGPG condenses the leaching of heavy metal ions lower than the regulatory limits, categorizing it as a non-hazardous material. In addition, WGPG is a viable binder for better sustainability compared to OPC.

8.2 Perceptions

For a better understanding of the performance and applications of WGPG, further studies are essential on the following aspects:

- Effect of feasible oxide compositions of waste glass on the mechanical properties of WGPG.
- Assessing the viable extent of reducing the usage of Na_2SiO_3 with WGP.
- Development of new testing methods for assessing the long-term ASR of WGPG.
- Supplementary studies on durability properties such as carbon resistance, chloride resistance, and salt attack resistance.
- Use of eco-friendly alkali material to enhance the sustainability of geopolymer material.
- Advanced sustainable studies on WGPG using comprehensive life-cycle analysis and life-cycle cost analysis.

Acknowledgements This study was carried out at the National Institute of Technology Rourkela, India, under the authority of the Ministry of Human Resource and Development, Government of India. Further, the authors acknowledge all the researchers whose works are used for the present review.

Author Contributions Datla Neeraj Varma: conceptualization, methodology, investigation, validation, writing—original draft preparation. Suresh Prasad Singh: Investigation, supervision, writing—review and editing.

Data Availability Data sharing not applicable to this article as no datasets were generated or analyzed during the present study.

Declarations

Consent for Publication All the authors confirm the consent for publication.

Competing Interests The authors declare no competing interests.

References

1. Jiang X, Xiao R, Ma Y et al (2020) Influence of waste glass powder on the physico-mechanical properties and microstructures of fly ash-based geopolymer paste after exposure to high temperatures. Constr Build Mater 262:120579. https://doi.org/10.1016/j.conbuildmat.2020.120579
2. Garside M (2021) Glass containers and bottles global production volume 2020 & 2026. In: Statista. https://www.statista.com/statistics/700260/glass-bottles-and-containers-production-volume-worldwide. Accessed 5 Mar 2023
3. Xiao R, Huang B, Zhou H et al (2022) A state-of-the-art review of crushed urban waste glass used in OPC and AAMs (geopolymer): Progress and challenges. Clean Mater 4:100083. https://doi.org/10.1016/j.clema.2022.100083
4. Zhang Y, Xiao R, Jiang X et al (2020) Effect of particle size and curing temperature on mechanical and microstructural properties of waste glass-slag-based and waste glass-fly ash-based geopolymers. J Clean Prod 273:122970. https://doi.org/10.1016/j.jclepro.2020.122970
5. Dadsetan S, Siad H, Lachemi M, Sahmaran M (2020) Extensive evaluation on the effect of glass powder on the rheology, strength, and microstructure of metakaolin-based geopolymer binders. Constr Build Mater 268:121168. https://doi.org/10.1016/j.conbuildmat.2020.121168
6. 20 Recycling Statistics for Eco-Conscious Canadians in 2022 (2022). https://reviewmoose.ca/blog/recycling-statistics/. Accessed 8 Mar 2023
7. Zhang L, Yue Y (2018) Influence of waste glass powder usage on the properties of alkali-activated slag mortars based on response surface methodology. Constr Build Mater 181:527–534. https://doi.org/10.1016/j.conbuildmat.2018.06.040
8. Manikandan P, Vasugi V, Siddika A et al (2021) A critical review of waste glass powder as an aluminosilicate source material for sustainable geopolymer concrete production. Silicon 13:1–26. https://doi.org/10.1007/s12633-020-00929-w
9. Dong W, Li W, Tao Z (2021) A comprehensive review on performance of cementitious and geopolymeric concretes with recycled waste glass as powder, sand or cullet. Resour Conserv Recycl 172:105664. https://doi.org/10.1016/j.resconrec.2021.105664
10. Sharholy M, Ahmad K, Mahmood G, Trivedi RC (2008) Municipal solid waste management in Indian cities - a review. Waste Manag 28:459–467. https://doi.org/10.1016/j.wasman.2007.02.008
11. Nandy B, Sharma G, Garg S et al (2015) Recovery of consumer waste in India - a mass flow analysis for paper, plastic and glass and the contribution of households and the informal sector. Resour Conserv Recycl 101:167–181. https://doi.org/10.1016/j.resconrec.2015.05.012
12. Solid waste diversion and disposal (2022) . https://www.canada.ca/en/environment-climate-change/services/environmental-indicators/solid-waste-diversion-disposal.html. Accessed 8 Mar 2023
13. Xiao R, Ma Y, Jiang X et al (2020) Strength, microstructure, efflorescence behavior and environmental impacts of waste glass geopolymers cured at ambient temperature. J Clean Prod 252:119610. https://doi.org/10.1016/j.jclepro.2019.119610
14. Duxson PJL, Lukey GC, van Deventer JSJ (2007) The role of inorganic polymer technology in the development of "green concrete." Cem Concr Res 37:1590–1597. https://doi.org/10.1016/j.cemconres.2007.08.018
15. Davidovits J (1991) Geopolymers - Inorganic polymeric new materials. J Therm Anal 37:1633–1656. https://doi.org/10.1007/BF01912193
16. Davidovits J, Davidovics M, Davidovits N (1994) Process for obtaining a geopolymeric alumno-slicate and products thus obtained. United States Patent, No. 5,342,595, Aug. 30, 1994
17. Assaedi H, Shaikh FUA, Low IM (2016) Effect of nano-clay on mechanical and thermal properties of geopolymer. J Asian Ceram Soc 4:19–28. https://doi.org/10.1016/j.jascer.2015.10.004
18. Okoye FN, Durgaprasad J, Singh NB (2016) Effect of silica fume on the mechanical properties of fly ash based-geopolymer

concrete. Ceram Int 42:3000–3006. https://doi.org/10.1016/j.ceramint.2015.10.084
19. Adak D, Sarkar M, Mandal S (2017) Structural performance of nano-silica modified fly-ash based geopolymer concrete. Constr Build Mater 135:430–439. https://doi.org/10.1016/j.conbuildmat.2016.12.111
20. Degefu DM, Liao Z, Berardi U, Labbé G (2022) The dependence of thermophysical and hygroscopic properties of macro-porous geopolymers on Si/Al. J Non Cryst Solids 582:121432. https://doi.org/10.1016/j.jnoncrysol.2022.121432
21. Aziz IH, Al Bakri Abdullah MM, Heah CY, Liew YM (2020) Behaviour changes of ground granulated blast furnace slag geopolymers at high temperature. Adv Cem Res 32:465–475. https://doi.org/10.1680/JADCR.18.00162
22. Hamid Abed M, Abbas IS, Canakci H (2022) Influence of mechanochemical activation on the rheological, fresh, and mechanical properties of one-part geopolymer grout. Adv Cem Res:1–38. https://doi.org/10.1680/JADCR.21.00205
23. Zhang YS, Sun W, Li ZJ (2005) Hydration process of potassium polysialate (K-PSDS) geopolymer cement. Adv Cem Res 17:23–28. https://doi.org/10.1680/adcr.2005.17.1.23
24. Das D, Rout PK (2023) Synthesis of inorganic polymeric materials from industrial solid waste. Silicon 15:1771–1791. https://doi.org/10.1007/s12633-022-02116-5
25. Nadeem M, Ilyas S, Haq EU et al (2022) Improved water retention and positive behavior of silica based geopolymer utilizing granite powder. Silicon 14:2337–2349. https://doi.org/10.1007/s12633-021-01047-x
26. Radhika N, Sathish M (2022) A review on Si-based ceramic matrix composites and their infiltration based techniques. Springer, Netherlands
27. Awoyera P, Adesina A (2019) A critical review on application of alkali activated slag as a sustainable composite binder. Case Stud Constr Mater 11:e00268. https://doi.org/10.1016/j.cscm.2019.e00268
28. Driouich A, Chajri F, El Hassani SEA et al (2020) Optimization synthesis geopolymer based mixture metakaolin and fly ash activated by alkaline solution. J Non Cryst Solids 544:120197. https://doi.org/10.1016/j.jnoncrysol.2020.120197
29. Sivasakthi M, Jeyalakshmi R, Rajamane NP, Jose R (2018) Thermal and structural micro analysis of micro silica blended fly ash based geopolymer composites. J Non Cryst Solids 499:117–130. https://doi.org/10.1016/j.jnoncrysol.2018.07.027
30. Bouguermouh K, Bouzidi N, Mahtout L et al (2017) Effect of acid attack on microstructure and composition of metakaolin-based geopolymers: the role of alkaline activator. J Non Cryst Solids 463:128–137. https://doi.org/10.1016/j.jnoncrysol.2017.03.011
31. Wang Y, Wang X, Lou Y et al (2022) Effect of mechanical activation on reaction mechanism of one-part fly ash/slag-based geopolymer. Adv Cem Res. https://doi.org/10.1680/JADCR.21.00033
32. Poowancum A, Aengchuan P (2022) Utilisation of low-reactivity fly ash for fabricating geopolymer materials. Adv Cem Res:1–8. https://doi.org/10.1680/JADCR.21.00025
33. Zhang J, Li S, Li Z et al (2021) Workability and microstructural properties of red-mud-based geopolymer with different particle sizes. Adv Cem Res 33:210–223. https://doi.org/10.1680/JADCR.19.00085
34. Liu L, Liu H, Xu Y et al (2022) Chemical deformation and mass change of metakaolin-based geopolymer grouting material in sulfate environment. Adv Cem Res. https://doi.org/10.1680/JADCR.21.00090
35. Khater HM (2014) Studying the effect of thermal and acid exposure on alkaliactivated slag geopolymer. Adv Cem Res 26:1–9. https://doi.org/10.1680/adcr.11.00052
36. Tome S, Nana A, Kaze CR et al (2022) Resistance of alkali-activated blended volcanic ash-MSWI-FA mortar in sulphuric acid and artificial seawater. Silicon 14:2687–2694. https://doi.org/10.1007/s12633-021-01055-x
37. Papa E, Medri V, Landi E et al (2014) Production and characterization of geopolymers based on mixed compositions of metakaolin and coal ashes. Mater Des 56:409–415. https://doi.org/10.1016/j.matdes.2013.11.054
38. Cyr M, Idir R, Poinot T (2012) Properties of inorganic polymer (geopolymer) mortars made of glass cullet. J Mater Sci 47:2782–2797. https://doi.org/10.1007/s10853-011-6107-2
39. Christiansen MU (2013) An investigation of waste glass-based geopolymers supplemented with alumina. Diss Michigan Technol Univ 21:1–416
40. Maraghechi H, Salwocki S, Rajabipour F (2017) Utilisation of alkali activated glass powder in binary mixtures with Portland cement, slag, fly ash and hydrated lime. Mater Struct Constr 50:16. https://doi.org/10.1617/s11527-016-0922-5
41. Zhang S, Keulen A, Arbi K, Ye G (2017) Waste glass as partial mineral precursor in alkali-activated slag/fly ash system. Cem Concr Res 102:29–40. https://doi.org/10.1016/j.cemconres.2017.08.012
42. Samarakoon MH, Ranjith PG, De Silva VRS (2020) Effect of soda-lime glass powder on alkali-activated binders: rheology, strength and microstructure characterization. Constr Build Mater 241:118013. https://doi.org/10.1016/j.conbuildmat.2020.118013
43. Rashidian-Dezfouli H, Rangaraju PR, Kothala VSK (2018) Influence of selected parameters on compressive strength of geopolymer produced from ground glass fiber. Constr Build Mater 162:393–405. https://doi.org/10.1016/j.conbuildmat.2017.09.166
44. Sadat MR, Bringuier S, Muralidharan K et al (2016) An atomistic characterization of the interplay between composition, structure and mechanical properties of amorphous geopolymer binders. J Non Cryst Solids 434:53–61. https://doi.org/10.1016/j.jnoncrysol.2015.11.022
45. Idir R, Cyr M, Tagnit-Hamou A (2013) Role of the nature of reaction products in the differing behaviours of fine glass powders and coarse glass aggregates used in concrete. Mater Struct Constr 46:233–243. https://doi.org/10.1617/s11527-012-9897-z
46. Puertas F, Torres-Carrasco M (2014) Use of glass waste as an activator in the preparation of alkali-activated slag. Mechanical strength and paste characterisation. Cem Concr Res 57:95–104. https://doi.org/10.1016/j.cemconres.2013.12.005
47. Rakhimova NR, Rakhimov RZ (2019) Toward clean cement technologies: a review on alkali-activated fly-ash cements incorporated with supplementary materials. J Non Cryst Solids 509:31–41. https://doi.org/10.1016/j.jnoncrysol.2019.01.025
48. Mendes BC, Pedroti LG, Vieira CMF et al (2022) Evaluation of eco-efficient geopolymer using chamotte and waste glass-based alkaline solutions. Case Stud Constr Mater 16:e00847. https://doi.org/10.1016/j.cscm.2021.e00847
49. Liu Y, Shi C, Zhang Z, Li N (2019) An overview on the reuse of waste glasses in alkali-activated materials. Resour Conserv Recycl 144:297–309. https://doi.org/10.1016/j.resconrec.2019.02.007
50. Shi C, Zheng K (2007) A review on the use of waste glasses in the production of cement and concrete. Resour Conserv Recycl 52:234–247. https://doi.org/10.1016/j.resconrec.2007.01.013
51. Wang WC, Chen BT, Wang HY, Chou HC (2016) A study of the engineering properties of alkali-activated waste glass material (AAWGM). Constr Build Mater 112:962–969. https://doi.org/10.1016/j.conbuildmat.2016.03.022
52. Bobirică C, Shim JH, Pyeon JH, Park JY (2015) Influence of waste glass on the microstructure and strength of inorganic polymers. Ceram Int 41:13638–13649. https://doi.org/10.1016/j.ceramint.2015.07.160
53. Shevchenko VV, Kotsay GN (2020) Influence of glass powder additives on the hydration process of Portland cement. Glas Phys Chem 46:653–656. https://doi.org/10.1134/S1087659620060231

54. Long WJ, Lin C, Ye TH et al (2021) Stabilization/solidification of hazardous lead glass by geopolymers. Constr Build Mater 294:123574. https://doi.org/10.1016/j.conbuildmat.2021.123574
55. Sobolev K, Türker P, Soboleva S, Iscioglu G (2007) Utilization of waste glass in ECO-cement: strength properties and microstructural observations. Waste Manag 27:971–976. https://doi.org/10.1016/j.wasman.2006.07.014
56. Liu G, Florea MVA, Brouwers HJH (2019) Waste glass as binder in alkali activated slag–fly ash mortars. Mater Struct Constr 52:1–12. https://doi.org/10.1617/s11527-019-1404-3
57. Ahmad J, Zhou Z (2023) Strength and durability properties of waste glass based self compacting concrete: a review. Silicon. https://doi.org/10.1007/s12633-023-02413-7
58. Mallum I, Abdul AR, Lim NHAS, Omolayo N (2022) Sustainable utilization of waste glass in concrete: a review. Silicon 14:3199–3214. https://doi.org/10.1007/s12633-021-01152-x
59. El-Shamy TM, Pantano CG (1977) Decomposition of silicate glasses in alkaline solutions. Nature 266:704–706
60. El-Naggar MR, El-Dessouky MI (2017) Re-use of waste glass in improving properties of metakaolin-based geopolymers: mechanical and microstructure examinations. Constr Build Mater 132:543–555. https://doi.org/10.1016/j.conbuildmat.2016.12.023
61. Yoo DY, Lee Y, You I et al (2022) Utilization of liquid crystal display (LCD) glass waste in concrete: a review. Cem Concr Compos 130:104542. https://doi.org/10.1016/j.cemconcomp.2022.104542
62. Kouassi SS, Andji J, Bonnet JP, Rossignol S (2010) Dissolution of waste glasses in high alkaline solutions. Ceram - Silikaty 54:235–240
63. Vafaei M, Allahverdi A (2017) High strength geopolymer binder based on waste-glass powder. Adv Powder Technol 28:215–222. https://doi.org/10.1016/j.apt.2016.09.034
64. Wang CC, Wang HY, Chen BT, Peng YC (2017) Study on the engineering properties and prediction models of an alkali-activated mortar material containing recycled waste glass. Constr Build Mater 132:130–141. https://doi.org/10.1016/j.conbuildmat.2016.11.103
65. Shoaei P, Ameri F, Reza Musaeei H et al (2020) Glass powder as a partial precursor in Portland cement and alkali-activated slag mortar: a comprehensive comparative study. Constr Build Mater 251:118991. https://doi.org/10.1016/j.conbuildmat.2020.118991
66. Si R, Guo S, Dai Q, Wang J (2020) Atomic-structure, microstructure and mechanical properties of glass powder modified metakaolin-based geopolymer. Constr Build Mater 254:119303. https://doi.org/10.1016/j.conbuildmat.2020.119303
67. Das SK, Shrivastava S (2022) Durability analysis and optimization of a binary system of waste cement concrete and glass-based geopolymer mortar. J Mater Cycles Waste Manag 24:1281–1294. https://doi.org/10.1007/s10163-022-01400-1
68. Varma DN, Singh SP (2023) Recycled waste glass as precursor for synthesis of slag-based geopolymer. Mater Today Proc. https://doi.org/10.1016/j.matpr.2023.03.516
69. Lu JX, Poon CS (2018) Use of waste glass in alkali activated cement mortar. Constr Build Mater 160:399–407. https://doi.org/10.1016/j.conbuildmat.2017.11.080
70. Li L, Lu JX, Zhang B, Poon CS (2020) Rheology behavior of one-part alkali activated slag/glass powder (AASG) pastes. Constr Build Mater 258:120381. https://doi.org/10.1016/j.conbuildmat.2020.120381
71. Manikandan P, Natrayan L, Duraimurugan S, Vasugi V (2022) Influence of waste glass powder as an aluminosilicate precursor in synthesizing ternary blended alkali-activated binder. Silicon. https://doi.org/10.1007/s12633-021-01533-2
72. İpek S (2022) Macro and micro characteristics of eco-friendly fly ash-based geopolymer composites made of different types of recycled sand. J Build Eng 52:104431. https://doi.org/10.1016/j.jobe.2022.104431
73. J-xin Lu, Z-hua Duan, Poon CS (2017) Combined use of waste glass powder and cullet in architectural mortar. Cem Concr Compos 82:34–44. https://doi.org/10.1016/j.cemconcomp.2017.05.011
74. Samantasinghar S, Singh SP (2018) Effect of synthesis parameters on compressive strength of fly ash-slag blended geopolymer. Constr Build Mater 170:225–234. https://doi.org/10.1016/j.conbuildmat.2018.03.026
75. Palacios M, Puertas F (2011) Effectiveness of mixing time on hardened properties of waterglass-activated slag pastes and mortars. ACI Mater J 108:73–78. https://doi.org/10.14359/51664218
76. Mithanthaya IR, Marathe S, Rao NBS, Bhat V (2017) Influence of superplasticizer on the properties of geopolymer concrete using industrial wastes. Mater Today Proc 4:9803–9806. https://doi.org/10.1016/j.matpr.2017.06.270
77. Toniolo N, Taveri G, Hurle K et al (2017) Fly-ash-based geopolymers: how the addition of recycled glass or red mud waste influences the structural and mechanical properties. J Ceram Sci Technol 8:411–419. https://doi.org/10.4416/JCST2017-00053
78. Toniolo N, Rincón A, Roether JA et al (2018) Extensive reuse of soda-lime waste glass in fly ash-based geopolymers. Constr Build Mater 188:1077–1084. https://doi.org/10.1016/j.conbuildmat.2018.08.096
79. Yoo DY, Lee SK, You I et al (2022) Development of strain-hardening geopolymer mortar based on liquid-crystal display (LCD) glass and blast furnace slag. Constr Build Mater 331:127334. https://doi.org/10.1016/j.conbuildmat.2022.127334
80. Derinpinar AN, Karakoç MB, Özcan A (2022) Performance of glass powder substituted slag based geopolymer concretes under high temperature. Constr Build Mater 331:127318. https://doi.org/10.1016/j.conbuildmat.2022.127318
81. Sethi H, Bansal PP, Sharma R (2019) Effect of addition of GGBS and glass powder on the properties of geopolymer concrete. Iran J Sci Technol - Trans Civ Eng 43:607–617. https://doi.org/10.1007/s40996-018-0202-4
82. Zribi M, Samet B, Baklouti S (2019) Effect of curing temperature on the synthesis, structure and mechanical properties of phosphate-based geopolymers. J Non Cryst Solids 511:62–67. https://doi.org/10.1016/j.jnoncrysol.2019.01.032
83. Verma M, Dev N (2022) Effect of liquid to binder ratio and curing temperature on the engineering properties of the geopolymer concrete. Silicon 14:1743–1757. https://doi.org/10.1007/s12633-021-00985-w
84. Ojha A, Aggarwal P (2023) Development of mix design guidelines for low calcium fly ash-based geopolymer concrete – a quantitative approach. Silicon 15:3681–3694. https://doi.org/10.1007/s12633-023-02299-5
85. Toniolo N (2019) Novel geopolymers incorporating silicate waste. Thesis report, Friedrich-Alexander-University (FAU)
86. Martinez-Lopez R, Ivan Escalante-Garcia J (2016) Alkali activated composite binders of waste silica soda lime glass and blast furnace slag: strength as a function of the composition. Constr Build Mater 119:119–129. https://doi.org/10.1016/j.conbuildmat.2016.05.064
87. Wang W, Noguchi T (2020) Alkali-silica reaction (ASR) in the alkali-activated cement (AAC) system: a state-of-the-art review. Constr Build Mater 252:119105. https://doi.org/10.1016/j.conbuildmat.2020.119105
88. He P, Zhang B, Lu JX, Poon CS (2020) A ternary optimization of alkali-activated cement mortars incorporating glass powder, slag and calcium aluminate cement. Constr Build Mater 240:117983. https://doi.org/10.1016/j.conbuildmat.2019.117983
89. He P, Zhang B, Lu JX, Poon CS (2021) Reaction mechanisms of alkali-activated glass powder-ggbs-CAC composites. Cem Concr Compos 122:104143. https://doi.org/10.1016/j.cemconcomp.2021.104143

90. Hui-Teng N, Cheng-Yong H, Yun-Ming L et al (2022) Comparison of thermal performance between fly ash geopolymer and fly ash-ladle furnace slag geopolymer. J Non Cryst Solids 585:121527. https://doi.org/10.1016/j.jnoncrysol.2022.121527
91. Abdulkareem OA, Mustafa Al Bakri AM, Kamarudin H et al (2014) Effects of elevated temperatures on the thermal behavior and mechanical performance of fly ash geopolymer paste, mortar and lightweight concrete. Constr Build Mater 50:377–387. https://doi.org/10.1016/j.conbuildmat.2013.09.047
92. Xiao R, Jiang X, Wang Y et al (2021) Experimental and thermodynamic study of alkali-activated waste glass and calcium sulfoaluminate cement blends: shrinkage, efflorescence potential, and phase assemblages. J Mater Civ Eng 33:1–14. https://doi.org/10.1061/(asce)mt.1943-5533.0003941
93. Bobirică C, Shim JH, Park JY (2018) Leaching behavior of fly ash-waste glass and fly ash-slag-waste glass-based geopolymers. Ceram Int 44:5886–5893. https://doi.org/10.1016/j.ceramint.2017.12.085